JOURNAL OF MATERIALS SCIENCE 11 (1976) 2087–2098

Structure, formation mechanisms and kinetics of reaction-bonded silicon nitride

HAMLIN M. JENNINGS*, MARC H. RICHMAN
Division of Engineering, Brown University, Providence, Rhode Island, USA

This paper reports on models which have been developed to explain the formation mechanism and kinetics of the major microconstituents of reaction-bonded silicon nitride. These models are based on information obtained from a detailed microstructural study during various stages of reaction and a knowledge of the reaction conditions which encourage formation of each particular microconstituent. It has become clear that there are at least two independent mechanisms and that they are governed by independent rate laws. The kinetics of nitridation of a silicon compact is, therefore, the superposition of at least two independent rate laws. Experimental evidence obtained thus far is in good agreement with this hypothesis.

1. Introduction

Silicon nitride possesses very good properties for high temperature engineering applications. As a result, an extensive effort to develop useful fabrication techniques was initiated in the early 1960s at the Admiralty Materials Laboratory in England by Parr and co-workers [1, 2]. Since then, research has been conducted in Great Britain, the United States and recently in Germany [3]. Thermal shock resistance and high temperature creep, erosion and corrosion resistance make silicon nitride attractive for such components of gas turbine engines as rotors, stators, heat exchangers and combustion chambers. Reaction-bonded silicon nitride has the advantage of maintaining its bulk dimensions during nitridation, which allows it to be easily fabricated into complex shapes. Progress has been made in the effort to increase its strength and creep resistance, with strengths in excess of 350 MPa (50×10^3 psi) being reported [4]. Correlations have been made between degree of reaction, density and strength [4–6], giving positive direction to research programs. Much of the work on the reaction-bonded material has been reviewed elsewhere [7–9].

There has, however, been great difficulty in understanding the formation mechanism and kinetics of nitridation. This confusion has been reflected in the literature [10, 11], where linear and logarithmic rates have been reported, and the conditions leading to the various kinetics have been difficult to reproduce and control. If real progress is to be made with the reaction-bonding technique, an understanding here is as necessary as the understanding of how density and degree of reaction are related to bulk properties. It will lead to a control of the microstructure and consequently control of the engineering properties.

The purpose of this paper is to illustrate the progress which has been made in the following areas: (1) establishing a detailed cause-effect relationship between processing conditions and microstructure, (2) developing models of the formation mechanism, and (3) inferring possible kinetic relationships. It is believed that this understanding will aid researchers to further develop reaction-bonded silicon nitride as a useful high temperature material.

2. Experimental

2.1. Fabrication

This investigation studied many variables, with over 90 samples being nitrided, one at a time, subject to a wide variety of conditions. Starting particle size and purity were varied between batches of nominally 99% pure (−200 mesh) and

* Present address: Department of Metallurgy and Materials Science, University of Cape Town, South Africa.

99.99% pure (−325 mesh) silicon powder. Table I shows the chemical and size analysis of the two grades of powder used. For some experiments the 99% pure powder was sieved to −325 mesh so that a simple comparison between purities can be made. Ultra fine particle size (mean size ~5 μm) was obtained by ball milling. The powder was maintained and handled in a dry nitrogen atmosphere. Cation impurities were checked for spectroscopically, and sieves and scanning electron microscopy were used to check particle size.

TABLE I (a) Chemical analysis of "−200 mesh" Si powder

Element	Amount (%)	Element	Amount (%)
B	0.001–0.01	Cr	0.001
Al	0.01–1.0	Mn	1.0
Ca	0.01–0.1	Fe	1.0–10.0
Ti	0.01–0.1	Ni	0.01–0.1
V	0.01	Zr	0.001–0.01
		Ag	< 0.0001

TABLE I (b) Particle size distribution for "−200 mesh" Si powder

Mesh size	Particle size (μm)	%
+ 50	> 297	0.0
+ 100	> 149	0.11
+ 200	> 74	17.17
−200	< 74	82.47

TABLE I (c) Chemical analysis of "−400 mesh" Si powder

Element	Amount (%)	Element	Amount (%)
B	0.001–0.01	Ti	0.0001–0.001
Sb	0.01–0.1	Cr	0.01–0.1
Mg	0.0001–0.001	Mn	0.01–1.0
Al	< 0.0001	Fe	0.1–1.0
Ca	0.001–0.01	Cu	0.0001–0.01
		Ag	< 0.0001

TABLE I (d) Particle size distribution for "−400 mesh" Si powder

Mesh	Particle size (μm)	%
+ 50	> 297	0.0
+ 100	> 149	1.14
+ 200	> 74	12.30
−200	< 74	86.02

A cylindrical compact was formed using a split steel die 2.54 cm diameter. About 8 g of powder and usually a temporary binder (e.g. acetone) were pressed under 29 to 44 MPa (4.3 to 6.4 x 10^3 psi). The "green" compact was then placed in a vacuum desiccator to draw off any volatile material. The density was calculated from weight and volume measurements and constituted one variable which was held relatively constant at 1.5 g cm^{-3} (correlations [4–6] have already been made between density and strength and one of our goals was to establish a correlation between microstructure and strength).

The nitridation process was carried out in a vertical tube furnace, heated with a silicon carbide element surrounding the reaction chamber which was made of recrystallized aluminium oxide ~3 cm diameter. The sample contacted only a block of silicon nitride used as a support. High purity nitrogen gas containing a maximum of 0.0008 mol % oxygen was dried by passing over P_2O_5 before entering the reaction chamber, where it was maintained at a slight positive pressure.

During nitridation the gas could be made to flow over the sample at rates anywhere between 0 and 350 $cm^3 min^{-1}$. Nitridation temperatures ranged from 1200 to 1600° C for times from several hours to several days. The rates of heating and cooling were automatically controlled* and varied from 30° C h^{-1} to several thousand °C min^{-1} (in the latter case the sample was abruptly lowered into the hot zone).

2.2. Specimen characterization

After nitridation, density was again calculated from weight and volume measurements and this, when compared to the "green" density, allowed the degree of reaction and per cent porosity to be calculated.

The specimen was then cut into several pieces using a diamond saw on a Micro-matic wafering machine. The pieces were used to perform the following tests: (1) powder X-ray diffraction to determine the relative amounts of alpha and beta Si_3N_4, unreacted silicon, and any other impurity phases. (2) Optical, transmission and scanning electron microscopy to characterize the microstructure. Optical samples were polished, TEM samples were ion-beam milled, and the SEM was used to examine fracture surfaces which were coated with 100 to 200 Å of gold. Details of

* This does not account for the exothermic nature of the reaction which can cause substantial internal temperature rises in the specimens being nitrided.

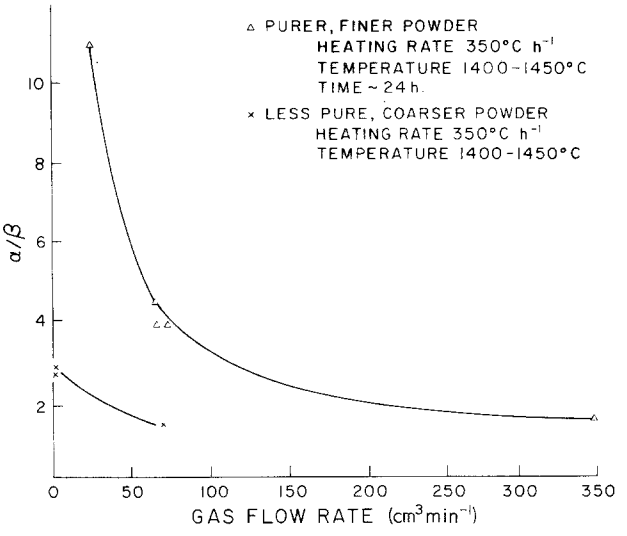

Figure 1 Ratio of α/β versus gas flow rate.

these procedures have been published elsewhere [12, 13]. (3) Although not of great import here, transverse rupture strength was determined by three-point bending.

3. Microstructure

The predominant microconstituents are alpha-phase needles, alpha-phase matte, and beta spikes. Each of these components has a distinct formation sequence and this, coupled with knowledge of the reaction conditions which encourage the formation of a particular microconstituent, supplies strong evidence regarding the mechanism and kinetics of formation. It should be emphasized, however, that because there are several competing rates, most processing conditions lead to several microconstituents. Using the results from a large number of experiments has enabled us to establish conditions which encourage the formation of a particular phase. These trends are presented in Table II. (Figs. 1 to 3 show more specific data, from which Table II was derived). It should be noted that for each datum point all conditions, except the one indicated, must be kept constant.

A detailed presentation of the microstructure is presented elsewhere [12] but in order to facilitate an understanding of the formation mechanism some micrographs will be presented here.

TABLE II Processing parameters encouraging specific morphologies

Microconstituent	Time (h)	Temperature (° C)	Heating rate	Gas flow rate	Comment
α needle	< 24	< 1400 seems to favour needles	300° C h^{-1}	–	observed in a majority of samples particularily less pure
β blades	> 24	> 1450	–	–	only observed when conditions are satisfied
α (fine) matte	–	< 1450	slow	no gas flow	use purer powder (finer)
β (coarse) matte	> 5	> 1450	rapid	fast gas flow	
β spikes	–	> 1450	rapid	fast gas flow	use less pure powder (coarser)
large pores	> 24	> 1450	rapid	–	
large unreacted grains	> 24	< 1400	300° C h^{-1}		

– indicates that evidence collected thus far does not indicate variable is important.

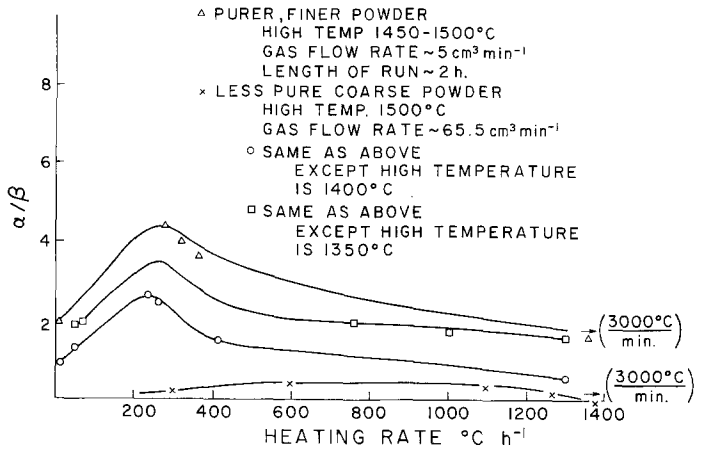

Figure 2 Ratio of α/β versus rate of heating.

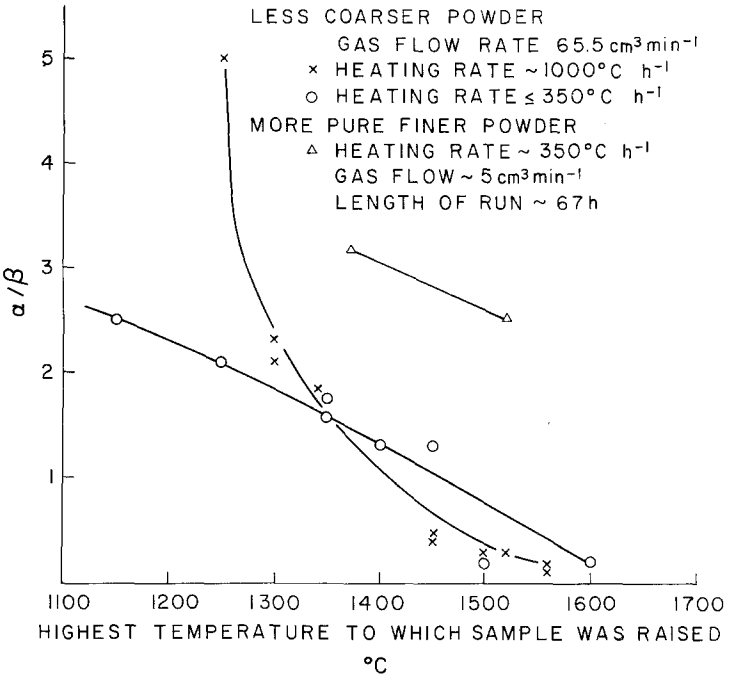

Figure 3 Ratio of α/β versus highest temperature to which sample was heated during reaction.

3.1. Alpha needles

Alpha needles appear in almost all samples but are particularly numerous when less pure starting powder is reacted in the temperature range of 1350 to 1400° C for several hours. The needles have a high aspect ratio (>25) and grow into the porosity of the original compact. Some of them are characterized by a small bead at the terminus (Fig. 4). Other needles are attached to large grains as shown in Fig. 5. Three types of alpha needles are observed in the transmission electron microscope. Again there are needles with and without beads on their terminus and some of these needles are clear while others have lines roughly perpendicular to the axis (Fig. 6 at C). It should be noted that most of the needles with lines do not have beads on their terminus. These lines have been attributed to impurity bands, interference bands and dislocations. Another type of needle can also be seen by the TEM and they have been characterized by Evans and Sharpe [14] as an inner crystalline core surrounded by an amorphous sheath as shown in Fig. 6 at B.

3.2. Alpha matte

The alpha silicon nitride can also manifest itself as a fine grained matte. The use of fine, pure powder and a heating rate of 300° Ch^{-1} to a temperature less that 1400° C with no gas flow

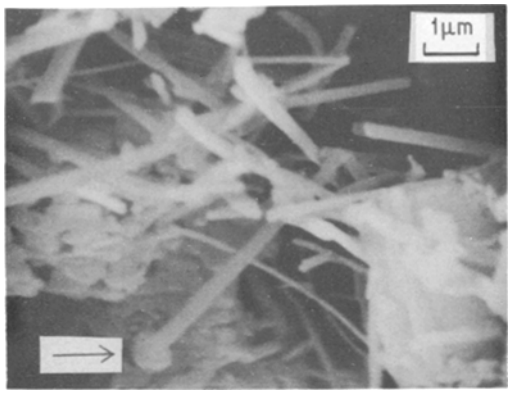

Figure 4 Needles of α, some of which have beads at terminus. SEM.

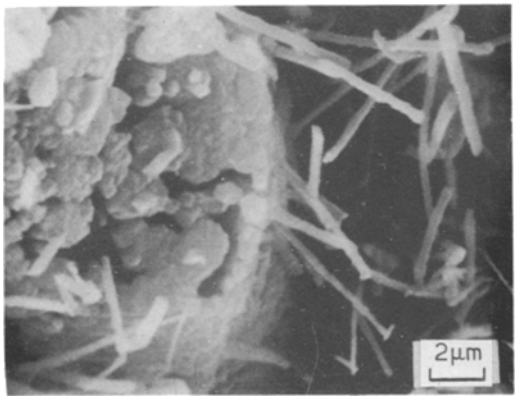

Figure 5 Photograph showing silicon that has been removed from unreacted grain as needles grow. SEM.

over the sample favors the formation of matte.

In the early stages of formation, the smallest silicon grains are the ones to react first and the product is often found around the larger grains, particularly in areas where the grains were formerly contiguous (Fig. 7). The product is very fine grained (<0.5 μm). As the reaction proceeds, all the smaller grains are consumed and the product fills the area between larger grains. Scanning electron micrographs show the matte advancing into grains with a characteristic porosity at the interface (Fig. 8). For still longer times the reaction leading to alpha-phase matte comes to a stop before the large grains of silicon have completely reacted to alpha.

3.3 Beta phase

The beta phase predominates when a sample made from less pure, coarser silicon (Table II) is heated rapidly in the presence of flowing nitrogen to a high temperature. In the initial stages of reaction, the beta phase forms on the surface of a grain and spikes grow (Fig. 9) in towards the centre of the grain. The grain size is much larger than the size of the alpha grains. As the reaction proceeds

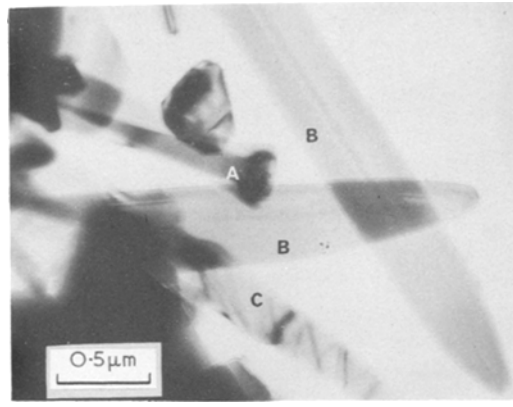

Figure 6 Transmission electron micrograph: A – α – needle with beads, B – α – needles with cores, C – α – needle with impurity bands.

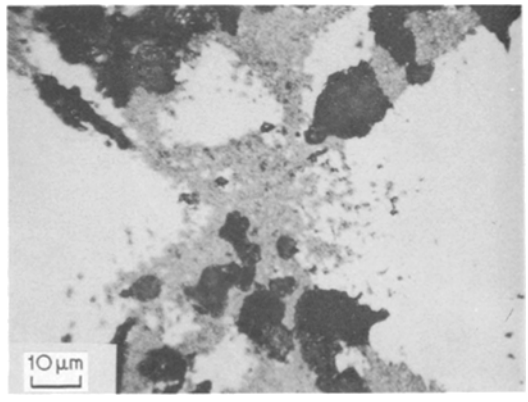

Figure 7 Optical micrograph showing initial stages of α-matte formation. Smallest grains react and fill in areas between larger grains.

the spikes become larger and fill up more and more of the original silicon grain (Fig. 10). Finally the spikes merge together into what appears to be one large reacted grain.

If, during this process, the temperature is raised and maintained at ~1500° C, i.e. well above the melting point of silicon, the silicon will melt and flow out leaving cavities which allow scanning electron micrographs of the spikes to be obtained

as if they had been growing into a void. Fig. 11 shows these spikes as they grow together into the void left by the melted-out grain.

4. Formation mechanism

4.1. Formation of the alpha phase

Several places of evidence support the idea [15] that the alpha phase is formed from the vapour

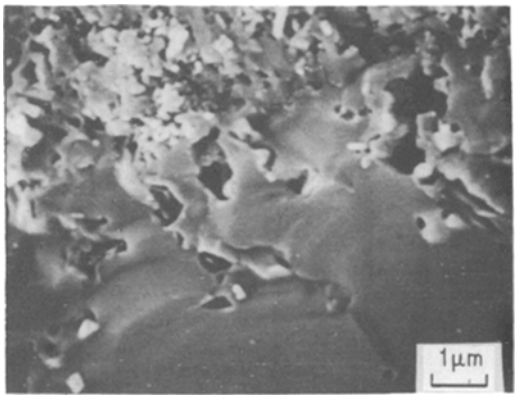

Figure 8 Alpha matte growing into grain of silicon. SEM.

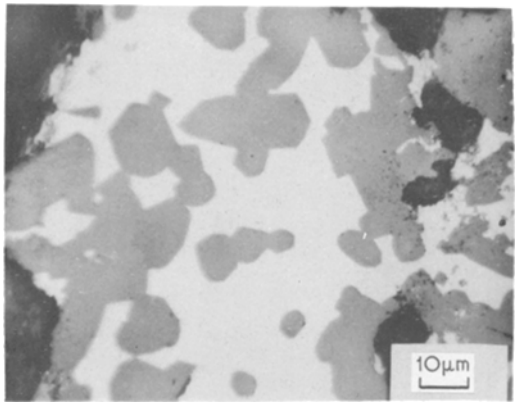

Figure 9 Initial stages of beta phase showing cross-section of grain of Si with β spikes running through it (not in plane of photograph).

state. They are (1) the detailed microstructure, (2) the fact that the percentage of alpha phase in the product is influenced by the introduction of oxygen, and (3) the fact that the percentage of alpha phase is influenced by the rate of flow of nitrogen gas over the sample.

Microscopic studies reveal that alpha matte often forms around the larger particles even though the smaller particles are the first to react. It is also observed that the bulk dimensions of a sample do not change during nitridation. From sintering theory it is known that the only way to transport material when a powder is heated, without changing the bulk dimensions, is surface diffusion and evaporation-condensation. Alpha matte has a very small grain size suggesting nucleation from the vapour phase and some of the alpha needles have beads on the terminus suggesting formation by means of a vapour–liquid–solid mechanism.

The influence of oxygen on the formation of alpha silicon nitride is well documented. Slight additions of oxygen [10] or water [16] greatly increase the percentage of alpha phase in the product. Messier and Wong [17] observed a weight loss (during thermogravimetric analysis experiments) when a small amount of oxygen was present in the nitrogen atmosphere. This was attributed to the formation of gaseous SiO. It has also been observed that even though oxygen encourages the formation of the alpha phase there can be virtually no oxygen in the resultant structure [18–20]. Taken together, these facts suggest

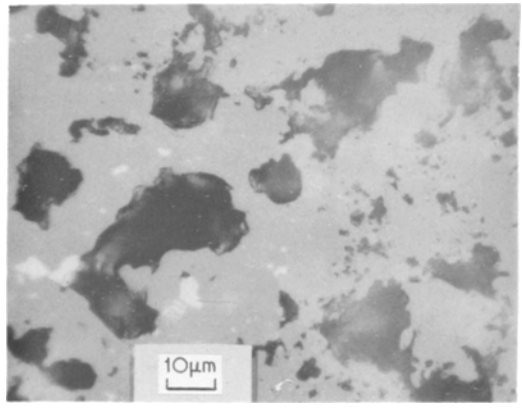

Figure 10 Micrograph shows spikes that are in contact and appear to be one reacted grain.

that the role of oxygen is to form gaseous SiO which in turn forms the alpha phase. The role of oxygen is simply that of encouraging the silicon to be carried to the reaction site in the vapour state and the oxygen need not necessarily enter the resulting structure, although in some cases it may.

There is a further possible role of oxygen. Gaseous nitrogen is not very reactive, but in the presence of a catalyst (usually a transition element) and at high temperature it will combine with oxygen to form NO which is considerably more reactive. In this way, the role of oxygen in the reaction between silicon and nitrogen may be

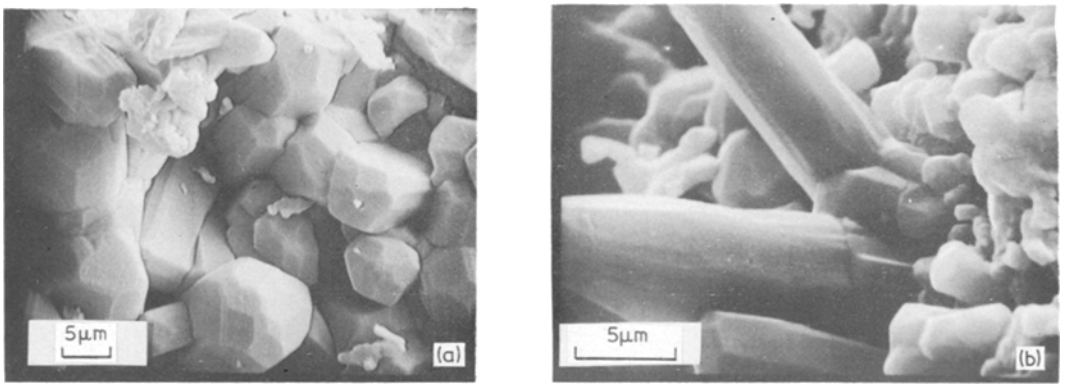

Figure 11 Fractograph showing spikes end-on (a) and from the side (b) as they continue to grow and merge together.

influenced by the presence or absence of other impurities as well as by temperature.

An inverse correlation has been made between the gas flow rate and percentage of alpha in the final product. A low percentage of alpha phase can be interpreted as a result of a gaseous intermediate being swept away by the flowing nitrogen and a high percentage of alpha phase is the result of the gas continuing to react in stagnant nitrogen.

In experiments using a flowing gas, a brown deposit sometimes appeared "downstream" from the specimen which, when analysed by X-ray diffraction, was found to be either one or a combination of $SiON_2$, SiO_2, Si or sometimes a material too amorphous for diffraction. This further supports the role of a gaseous phase in the reaction process.

When high purity single crystals are heated in a nearly oxygen-free nitrogen atmosphere, only the alpha phase forms. In this system, silicon can be carried to the reaction site as a vapour (by volatilization) without the presence of oxygen; and, if there is an over-riding reason which prevents the formation of the beta phase (which will be discussed in Section 5.3), alpha will be the predominant product. A high degree of crystallographic orientation ((0 0 1) basal plane parallel to (1 1 1) Si surface) was observed [21] in the growth of the alpha phase on single crystals. This further supports the idea that a vapour was involved and had a strong tendency to adsorb on preferred crystal planes.

4.1.1. Formation of alpha needles

Since it was first suggested by Gribkov *et al.* [23] it has been generally accepted that alpha needles form by a vapour–liquid–solid mechanism. The beads at the terminus of some needles often contain impurities such as Fe [11], which can lower the melting temperature of silicon as much as 200° C. Silicon is transported in the vapour phase to the bead where it condenses as a liquid. Nitrogen does not react with silicon in the liquid phase [16] and therefore it must react at the solid–liquid interface to form silicon nitride and thereby lengthen the needle. This process is schematically illustrated in Fig. 12. Under certain conditions the reaction may not proceed all the way to the centre of the needle leaving an unreacted inner core. This may explain how some needles were formed

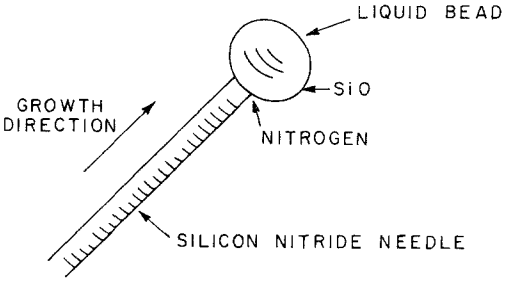

Figure 12 Schematic drawing showing growth of needles by V-L-S mechanism.

which appear to have unreacted silicon, which was once liquid, in their core [23, 24].

Many needles, however, have no beads attached to their ends but when examined they seem to be attached to larger grains (see Fig. 5). The same formation mechanism could operate if a "puddle" of liquid were to form on the surface of a larger grain and were to serve as the liquid in the VLS mechanism. When this happens, however, the

point of contact with the puddle will have to support the weight of the needle as it grows. At a certain point the needle could move, making an angle with the growth direction as illustrated in Fig. 13. This process could form low-angle grain boudaries or twins and may account for the lines running across some needles in the transmission electron micrographs. Also, impurities on the surface of the silicon grain could easily be trapped in the growing needle, further contributing to the observed lines. These lines have also been attributed to axial screw dislocations [23] and therefore further work is necessary in this area. Finally, the observation that the needles tend to grow at low temperatures could be explained by the need to keep the puddle at the root of the needle small and in contact with the needle. As the reaction continues, silicon would be supplied to the liquid puddle by diffusion from the bulk of the unreacted grain (see Fig. 5), creating channels and breaking up the larger grains.

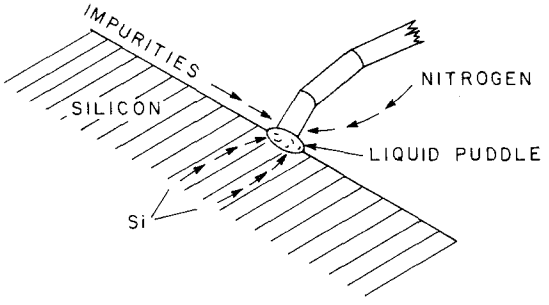

Figure 13 Schematic illustration showing possible mechanism for formation of needle with liquid phase on surface of silicon grain.

The amorphous sheath found around some needles is most probably an oxide layer formed after original needle growth.

4.1.2. Formation of alpha matte

The alpha matte is formed at the surface of the silicon particles, probably from the vapour phase. A detailed mechanism for the formation of the alpha matte has been proposed by Atkinson *et al.* [25] who suggest a sequence of events schematically illustrated in Fig. 14. They explain the fact that the overall dimensions of a sample remain unchanged during nitridation even though the volume of solid increases by 22% by postulating that no reaction takes place at the nitride–silicon interface. After a layer of nitride forms on the surface of a particle, silicon diffuses through this layer and reacts with nitrogen in the original voidage of the compact. As a consequence, vacancies are left behind in the unreacted silicon and combine to form pores. The process continues as nitrogen fills the pores and more silicon diffuses through the nitride to the surface of the particles. We are in complete agreement with these observations as discussed in Section 3.2. In particular, it explains the characteristic porosity and grain size which are observed in the alpha matte.

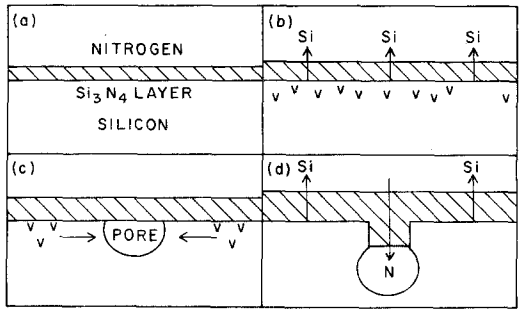

Figure 14 Schematic illustration of formation of alpha matte. (a) silicon is first covered with a layer of nitride, (b) Si migrates out and leaves vacancies behind, (c) vacancies condense to form a pore at the nitride-silicon interface and (d) nitride grows into pore which migrates into silicon grain. After Atkinson *et al.* [25].

4.2. Formation of the beta phase

A reaction mechanism for the formulation of the beta phase can be deduced from the microstructural study. As has been shown, spikes of the beta phase shoot into the grains of silicon and, as the reaction goes to completion, they coalesce and fuse together. The beta structure [26] has hexagonal tunnels 1.5 Å diameter running in the *c* direction. This allows nitrogen, which has a Van der Waals radius of 1.5 Å, to diffuse easily through

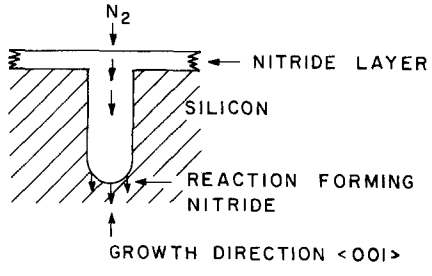

Figure 15 Schematic showing beta spike growing into silicon grain by diffusion of nitrogen down hexagonal tunnels to end of spike where reaction occurs.

the beta structure to the nitride–silicon interface. Nitrogen can easily escape so that trapped nitrogen will not alter the stoichiometry (any diffusion mechanism must allow for the release of nitrogen). A schematic illustration of the beta phase growing into silicon is shown in Fig. 15. This mechanism is a variation of the diffusion-barrier controlled mechanism first proposed by Wild *et al.* [15].

Because the silicon expands by 22% upon nitridation, space must be made available for the reaction to proceed. The introduction of porosity or the melting away of silicon could gain the needed space, but because the overall dimensions of the samples do not change there can be no growth into the particle when there is no available space. Therefore, the observed tendency for the percentage of beta to increase at high temperatures can be explained. Similarly, the presence of impurities in the powder will reduce the melting point of silicon and thereby encourage (because of contraction on melting and ability to flow) the formation of the beta modification. This is consistant with the observation, both elsewhere [11] and in this study, that impurities can increase the percentage of beta phase in the product.

Impurities in the nitrogen atmosphere could clog the hexagonal tunnels and make formation of beta difficult. This may be an indirect role of oxygen in encouraging the formation of alpha. If conditions favouring the formation of beta are present, the oxygen (or other impurities) could slow down the overall kinetics, as has been observed [27].

Finally, the high density of dislocations found in the beta structure as compared to the alpha structure could be explained by the fact that the beta forms in the solid state and the alpha grows from the vapour state.

5. Kinetics

Since the principal phases of reaction-bonded silicon nitride form by very different mechanisms, it would be surprising if they formed according to the same rate law. It is our contention that the overall rate of reaction results from the superposition of (at least) two independent rate types, with the various reaction conditions controlling the predominant mechanism for a single sample.

5.1. Alpha needles

At the initial stages of formation a bead or puddle composed of silicon forms on a large grain. The rate-controlling step is likely to be the rate at which nitrogen dissociates and since this may be accomplished in small, low energy steps, it may be quite rapid. As needles begin to form, the mechanism changes. In the case of needles growing from puddles, silicon is easily supplied to the liquid and the needles grow quite rapidly. In the case of needles growing with beads at their terminus, the rate of formation is probably dependent on the rate at which silicon is introduced into the vapour state and this is related to the ease of breaking silicon–silicon bonds. The activation energy is about 86 kcal mol^{-1} [28] and the silicon will probably condense rapidly because of its exothermicity.

Once the surface of the grains becomes coated with product (and this happens fairly quickly) the process is slowed down and complicated by the need for the diffusion of the reactants through the nitride layer. The rate of product formation becomes slower as the layer of nitride thickens and is also dependent on phase, grain size and morphology of nitride coating. It should be noted that the addition of impurities such as Fe can encourage the formation of alpha needles (if other conditions are correct as per Table II) and can, therefore, increase the rate of nitridation.

5.2. Alpha matte

After the very initial stages, the formation of alpha matte is also closely linked to the diffusion of the product through the nitride layer. Assuming that the rate-controlling step is the diffusion of reactants through the nitride layer, a first approximation of the rate law can be deduced by the following considerations.

The rate at which the thickness of a diffusion layer increases can be given by

$$\frac{dy}{dt} = \frac{Dk\Delta\eta}{y}, \qquad (1)$$

where $\Delta\eta$ is proportional to the driving force and usually a function of concentration, y = thickness, D = diffusion constant which depends exponentially on temperature, k = constant.

The driving force for any sintering process (in the absence of external pressure) is the free energy change which occurs when the neck between the particles thickens. This thickening lowers the solid–vapour surface area and increases the radius of curvature of the neck. (The well-known Kelvin equation expresses this concept.) It has been

suggested [29, 30] that the rate of neck growth for the vapour condensation method is given by

$$\frac{x^3}{r} = ct, \tag{2}$$

where t = time, x = neck radius, r = radius of spheres, c = temperature-dependent function. If the radius of the neck is considered to be inversely proportional to the driving force, it can be substituted for $\Delta\eta$ in Equation 1

$$\frac{dy}{dt} = \frac{DK'}{y(ctr)^{1/3}}. \tag{3}$$

Integrating:

$$y^2 = D'K''r^{-1/3}t^{2/3} \tag{4}$$

Now, if spherical particles are forming a nitride layer, then the volume of unreacted silicon is given (as suggested by Jander [31]) by

$$V = 4/3\,\pi(r-y)^3 \tag{5}$$

or

$$V = 4/3\,\pi r^3(1-\chi) \tag{6}$$

where χ = fraction already reacted. Combining Equations 5 and 6 gives:

$$y = r[1-(1-\chi)^{1/3}]. \tag{7}$$

This is valid, at least during the initial 75% of reaction. Then equating Equations 4 to 7 gives:

$$[1-(1-\chi)^{1/3}]^2 = \frac{D'K''t^{2/3}}{r^{7/3}} \tag{8}$$

Since other products besides alpha matte are forming simultaneously, Equation 8 can only be considered an approximate treatment. The results of a series of experiments with constant conditions except for time are given in Fig. 16. It has already been noted that many processing conditions affect the alpha to beta ratio and consequently only a few datum points have been taken with reaction time being the only variable. The agreement between experiment and theory is good, suggesting that the functional form of χ versus t is based on sound principles.

5.3. Beta phase

The pattern of growth for the beta phase is very different from that of the alpha phase. The development and growth of the beta spikes into the silicon grains suggests that the product is formed at the tip of the spike (i.e. the point penetrating into the silicon grain). Nitrogen must adsorb on the opposite end of the spike (i.e. the particle surface) and then diffuse down the length of the spike through the hexagonal tunnels to the silicon–silicon nitride interface.

The rate at which the beta phase forms and develops must depend on a number of conditions, including the probability of adsorption occurring. This phase will continue to grow as long as room for expansion inside the silicon grain exists. Without this necessary room the beta phase will not form in the solid state, which may explain the observed lack of beta phase when high purity single crystals of silicon are nitrided at $<1410°$ C

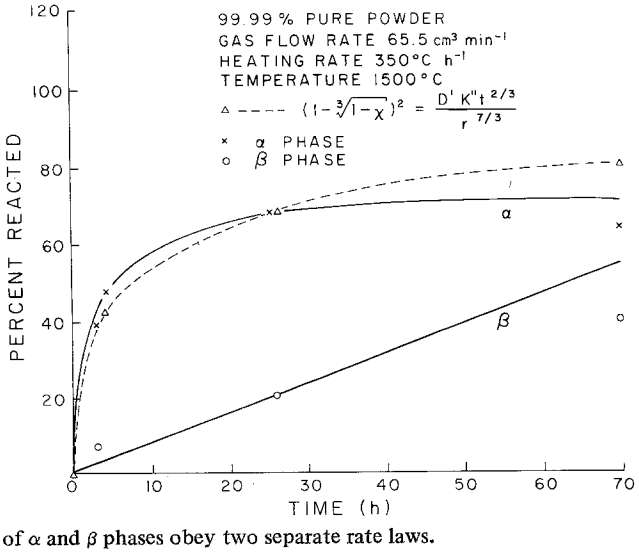

Figure 16 The formation of α and β phases obey two separate rate laws.

[21, 22]. If there is room for the beta spikes to grow, then the rate controlling step might be the adsorption and scission of the nitrogen. Alternatively, the rate of Si_3N_4 deposition at the end of the spike might be the rate-controlling step. Because of the large hexagonal tunnels offering easy nitrogen motion, diffusion is most likely not the rate-controlling step. The rate law, then, would be linear as is observed in Fig. 16, at least when the reaction temperature is above the temperature of fusion of the silicon. Deviation from expected rate laws after long reaction times is probably due to the fact that as the supply of unreacted silicon runs out, the formation of one phase will interfere with the kinetics of the other. This linear rate law has also been observed by Hüttinger [27] in his samples which were predominantly beta phase. The addition of impurities, particularly iron, to the silicon will lower the melting temperature of silicon and this will allow for the beta phase to grow more rapidly. It has been observed [11] that impurities increase the rate of nitridation and often this is accompanied by an increase in the percentage of beta in the product. Thus, under some conditions iron encourages the formation of alpha needles (as per Section 5.1) and under other conditions it can encourage the formation of the beta phase. If the reaction takes place at high temperature and long periods of time the latter case will probably dominate.

6. The effect of heating rate

The fact that the heating rate can have a significant effect on the rate of nitridation was first reported by Popper and Ruddlesden [32], but their observations were limited only to the total nitride formed and did not deal with the effect of heating rate on the alpha to beta ratio. This variable is very often not reported because it is an unusual variable to consider important and also because any effect that it does have is easily obscured by the large number of other variables which can alter the alpha to beta ratio. Many methods have been established for controlling the exotherm but this does not explain our observation that there is an optimum heating rate for the formation of the alpha phase.

In light of the ideas presented in this paper, however, it can be seen that heating rate must be an important variable. The alpha and beta phases form by different mechanisms and therefore have different activation energies. The relative rates are altered by initial grain size, purity, and temperature of reaction. Lower temperatures favour the formation of the alpha phase and higher temperatures favour the formation of the beta phase. Therefore, time (even a short time) spent at lower temperatures will influence the ratio of phases in the product.

Lower temperatures favour the formation of alpha matte because higher temperatures strongly favour the beta phase. A heating rate slow enough to allow the nucleation of alpha on a large protion of silicon grain surfaces will ensure the continued formation of alpha. If, however, the entire surface of silicon grains is covered with alpha matte (by very slow heating or long reaction times at low temperature), there will be no place for the unreacted silicon to expand upon further heating (coefficient of thermal expansion: $Si_3N_4 = 2.5 \times 10^{-6}\,^{\circ}C^{-1}$; $Si = 2.8 - 7.3 \times 10^{-6}\,^{\circ}C^{-1}$). Further heating will rupture the nitrided surface layer, exposing fresh unreacted silicon, which will react swiftly and exothermically, further raising the temperature and encouraging both the formation of beta and further rupture.

There is, therefore, a dependence of alpha to beta ratio on heating rate which may be explained (to a first approximation) by the formation mechanisms proposed in this paper. This dependence will exhibit a maximum alpha to beta ratio at a heating rate which is sufficiently slow to allow the nucleation of alpha but not so slow that the entire surface of the grains has started to react to the alpha modification.

7. Discussion

There is much work yet to be performed in order to refine the kinetic model proposed in this paper. Obviously there are exceptions to some of the ideas presented herein. Clancy [24] convincingly reports that under conditions of high temperature and pressure, beta phase crystals can form from the vapour. The observation of beta phase [21, 22] forming on high purity silicon crystals with impurities in the atmosphere suggests the possibility of other mechanisms operating. Alternative roles of oxygen such as the formation of NO, must be studied further.

The fact that there are several distinct formation mechanisms having separate rate-controlling steps, however, seems clear. The overall kinetics can be explained only by the super-

position of at least two independent rates. The resulting complex rate law is influenced by a large number of processing conditions, some of which have not yet been exploited. These arguments can be used to help understand many of the experimental results reported in the literature. The recent idea that nitridation takes place in two stages [33] can be interpreted as the rate of formation of the beta phase overtaking that of the alpha phase. The fact that reaction rate increases with increasing temperature and decreasing particle size [34] is also a straightforward interpretation of the proposed mechanisms. The favoured formation of the beta phase above the melting point of silicon [35] can be attributed to the fact that melting creates "room" by both its contraction upon melting and its ability to flow. Finally, the multiple role of many impurities can be more easily understood.

The properties of silicon nitride are dependent on density, degree of reaction, purity, and also on the microstructure. An understanding of the conditions which encourage and the kinetics which govern the formation of the various microconstituents will allow for the deliberate design of microstructure and a subsequent improvement of engineering properties.

Acknowledgement

The authors would like to thank Messrs Stephen Danforth, Joseph Fogarty and Mark Schreiner for help in accumulating data and valuable discussions leading to the development of ideas presented in this paper. They also would like to thank the U.S. Army Research Office for financial support of this research, by Grant DA-ARO-D-31-124-72-G183 (Project no. 10618-MC).

References

1. N. PARR, G. F. MARTIN and M. J. MAY, "Special Ceramics – 1959" Heywood, (London, 1960) p. 102.
2. N. PARR, British Patent 974 757 (1964).
3. E. C. VAN REUTH, in "Ceramics for High Performance Applications", edited by J. J. Burke, A. E. Gorum, and R. N. Katz (Brook Hill, Chestnut Hill, Mass, 1974) p. 1.
4. M. WASHBURN and H. BAUMGARTNER, *ibid*, p. 479.
5. A. MCLEAN, E. FISHER and R. BRATTON, A.M.M.R.C. Interim Report, Contract No. DAAG 46-71-C10162, 1 July–31 December 1972.
6. B. F. JONES and M. W. LINDLEY, *J. Mater. Sci.* **10** (1975) 967.
7. W. CROFT and I. CUTLER, E.R.O. Report No. 2–73, O.N.R. Report R-16-73 (July 1973).
8. J. EBINGTON, D. ROWCLIFFE and J. HENSHALL, *Powder Met. Int.* **7** (1975) 82.
9. D. MESSIER and M. MURPHY, A.M.M.R.C. Ms 75–1 (February 1975).
10. D. MESSIER, P. WONG and A. INGRAM, *J. Amer. Ceram. Soc.* **56** (1973) 171.
11. D. MESSIER and P. WONG, *ibid* **56** (1973) 480.
12. H. M. JENNINGS, S. C. DANFORTH and M. H. RICHMAN, *Metallography*, to be published.
13. S. C. DANFORTH and M. H. RICHMAN, *ibid.*
14. A. G. EVANS and J. V. SHARP, "Electron Microscopy and Structure of Materials", edited by G. Thomas, R. M. Fulrath, and R. M. Fisher (University of California Press, 1972) p. 1141.
15. S. WILD, P. GRIEVESON, and K. H. JACK, "Special Ceramics 5" edited by P. Popper (British Ceramic Research Association, Stoke-on-Trent, 1972) p. 271.
16. H. PRIEST, personal communication.
17. D. MESSIER and P. WONG, A.M.M.R.C. TR 74–1 (1974).
18. H. PRIEST, F. BURNS, G. PRIEST and E. SKAAR, *J. Amer. Ceram. Soc.* **56** (1973) 395.
19. A. EDWARDS, D. ELIAS, M. LINDLEY, A. ATKINSON and A. MOULSON, *J. Mater Sci.* **9** (1974) 516.
20. K. KIJIMA, K. KATO, Z. INOVE and H. TANAKA, *ibid* **10** (1975) 362.
21. R. B. GUTHRIE and F. L. RILEY, *Proc. Brit. Ceram. Soc.* **22** (1973) 275.
22. *idem, J. Mater, Sci.* **9** (1974) 1363.
23. V. GRIBKOV, V. SILAEV, B. SCHCHETANOV, E. UMANTSEU and A. ISAIKI, *Sov. Phys. – Crystsllogr.* **16** (1972) 852; translated from *Kristallografiya* **16** (1971) 982.
24. W. P. CLANCY, *The Microscope* **22** (1974) 279.
25. A. ATKINSON, P. J. LEATT, A. J. MOULSON and E. W. ROBERTS, *J. Mater Sci.* **9** (1974) 981.
26. D. S. THOMPSON and P. L. PRATT, "Science of Ceramics 3" edited by G. H. Stewart (Academic Press, London, 1967) p. 33.
27. K. HÜTTINGER, *High Temp. High Press.* **1** (1969) 221.
28. H. M. JENNINGS, J. O. EDWARDS and M. H. RICHMAN, *Inorg. Chim. Acta.*, to be published.
29. J. BURKE, General Electric Report No. 68-C-368 (November 1968).
30. G. KUCZNSKI, *Trans. Met. Soc. AIME.* **185** (1949) 169.
31. W. KINGERY, "Introduction to Ceramics", (Wiley New York, 1960) p. 338.
32. P. POPPER and S. N. RUDDLESDEN, *Trans, Brit. Ceram. Soc.* **60** (1961) 603.
33. D. CAMPOS-LORIZ and F. L. RILEY, *J. Mater. Sci.* **11** (1976) 195.
34. L. AMATO, D. MARTORANA and M. ROSSI, *Powder Met.* **18** (1975) 339.
35. A. G. EVANS and R. W. DAVIDGE, *J. Mater. Sci.* **5** (1970) 314.

Received 27 October 1975 and accepted 26 March 1976.